Infrared polarimetric sensing of oil on water

David B. Chenault*[a], Justin P. Vaden[a], Douglas A. Mitchell[b], Erik D. Demicco[b]

[a]Polaris Sensor Technologies, Inc., 200 Westside Square, Suite 320, Huntsville, AL 35801

[b]ExxonMobil Upstream Research Company, 22777 Springwoods Village Pkwy, Spring, TX 77389

ABSTRACT

Infrared polarimetry is an emerging sensing modality that offers the potential for significantly enhanced contrast in situations where conventional thermal imaging falls short. Polarimetric imagery leverages the different polarization signatures that result from material differences, surface roughness quality, and geometry that are frequently different from those features that lead to thermal signatures. Imaging of the polarization in a scene can lead to enhanced understanding, particularly when materials in a scene are at thermal equilibrium. Polaris Sensor Technologies has measured the polarization signatures of oil on water in a number of different scenarios and has shown significant improvement in detection through the contrast improvement offered by polarimetry. The sensing improvement offers the promise of automated detection of oil spills and leaks for routine monitoring and accidents with the added benefit of being able to continue monitoring at night. In this paper, we describe the instrumentation, and the results of several measurement exercises in both controlled and uncontrolled conditions.

Keywords: Polarization, infrared polarimetry, remote sensing, oil spill, oil on water, environmental monitoring

1. INTRODUCTION

The Deepwater Horizon incident is a well-known example of a large volume oil release (210,000,000 gallons) that had considerable impact on the marine and coastal environment and significant costs for the response and economic fallout. Lesser known are small volume spills (typically a few gallons that include natural, industrial, and recreational sources) that are regularly reported and archived by the EPA's National Response Center (NRC). For example, there were 30 smaller incidents reported between New Orleans and Mobile Bay in the month of July, 2016[1]. For relatively small spills, the response is heavily dependent on being able to locate the spill based on sporadic, sometimes non-specific reports, and to determine its size. With larger spills, a coordinated response team may be continually on site, but recovery operations are usually limited to day light hours and require updates on the spill location in the morning before recovery operations can begin, often causing hours of delay in oil recovery or mitigation. While infrared imaging is used in some cases, the thermal contrast between the oil and the water background is typically small and is further confounded by wave action. In all cases, the ability for personnel to quickly and easily detect oil on water is clearly needed for an appropriate, consistent, and cost effective response. The potential to automatically perform the same function could be a boon for oil responders and provide the opportunity for regular monitoring around drilling operations and facilities, transfer points, ports and harbors.

For many years, Polaris Sensor Technologies, Inc. has been developing imaging polarimetric sensors across the optical spectrum. In 2015, an oil pipeline in the vicinity of Santa Barbara, CA ruptured resulting in a spill into the Santa Barbara channel. An aerial survey of the oil spill with a Polaris infrared polarimeter resulted in significant improvement of oil detection over conventional thermal cameras even after cleanup efforts were conducted. With partial support from ExxonMobil Upstream Research Company (EMURC), we subsequently had the opportunity to test an infrared polarimeter at Ohmsett, the National Oil Spill Response Research & Renewable Energy Test Facility in northeast New Jersey. This test facility (Figure 1), maintained and operated by the U.S. Department of Interior's Bureau of Safety and Environmental Enforcement (BSEE), provides independent, objective performance testing of oil spill response equipment on a large scale and in as realistic environment as possible. At this test, a Polaris Pyxis® LWIR 640 infrared imaging polarimeter recorded a number of controlled spills to test its detection performance as a function of time of day and angle, oil type and thickness, and of the evolution and motion of several oil types in both flat water and in waves. In all cases, the infrared (IR) polarimetric data showed superior detection over that of thermal IR

Figure 1. Ohmsett – The National Oil Spill Response Research & Renewable Energy Test Facility.
Aerial photo provided by Ohmsett. Wave action photo provided by Polaris Sensor Technologies, Inc.

alone and enabled detection of even small amounts of oil on water throughout the night and in situations when the thermal imagery showed no contrast.

Pyxis is an infrared polarimetric sensor measuring not only the conventional thermal intensity of a scene but also the polarization magnitude and orientation of the plane of polarization. By measuring one or more parameters of the polarization ellipse, details can be extracted from a scene that are not readily apparent when using conventional thermal imagers alone. In the past, these measurements required large scientific instruments not readily applicable for hand-held use but the recent development of un-cooled, infrared sensor arrays has led to a significant reduction in size, weight, power and cost of high-performance polarimetric sensors. The Pyxis camera incorporates a micro filter array mounted in close contact to the microbolometer focal plane array (FPA). Pyxis is shown in Figure 2.

The strength and orientation of an infrared polarimetric signal relies on surface temperature, orientation, surface roughness, material properties, aspect angle to the sensor, down-welling sky radiance and terrestrial background radiance reflecting from the objects in the scene. Often times, the polarization signature of objects with different material properties is different than that of the surrounding background and most importantly, that difference is often present even when the intensity signature of the object of interest is in thermal equilibrium with the background[2,3]. In other words, the target can be completely invisible in the standard intensity image while at the same time exhibiting a strong polarimetric signature. Further, the fact that the polarization signal is based on emission, the polarization signal is available for day / night operations. It is this capability to provide polarization contrast resulting from material differences that we are exploiting here for oil on water detection.

In this paper, we describe the technology, the hardware and software, the tests, and finally the results of our testing at Ohmsett.

1.1 Technology Overview

The technology underlying the Pyxis sensor exploits the polarization of light in our environment, a fact that we use every day with our polarized sun glasses to reduce glare off the car in front of us in traffic. When ambient illumination is reflected off of an object, the reflected light becomes polarized. Likewise in the thermal infrared, light is polarized in both emission and reflection. Polarization is one of the fundamental quantities of light along with intensity and wavelength. However, these three quantities are independent of each other so that two beams of light with the same intensity and wavelength (or spectral distribution) can have very different polarization states. An imaging polarimeter measures these polarization states and provides additional information that exploits the polarization differences in the scene that are frequently different from the broadband intensity.

Figure 2. A Pyxis camera incorporates a micro filter array mounted in close contact to the COTS FPA.

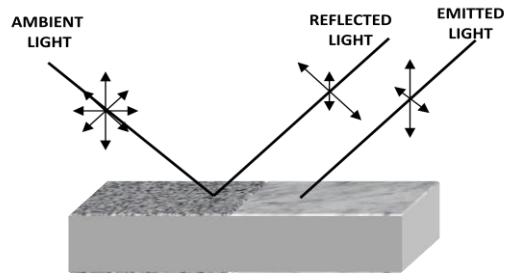

Figure 3. Phenomenology of polarization sensing. Emission and reflection of light from surfaces of different materials at different angles leads to a rich phenomenology for polarized light.

Figure 3 depicts some of the phenomenology that gives rise to polarization signatures in passive polarization imaging. The polarization in the scene depends on the angles of the surface normals relative to the sensor look angle and the surface optical characteristics. The larger the angle between the surface normal and the sensor look angle (the angle of incidence or AOI), the higher the polarization signal from that surface. The surface optical characteristics depend on the materials of the surface and other surface characteristics, such as roughness and presence of dirt and water. As the surface roughness increases, the polarization signal reflected or emitted from the surface decreases.

It is well known that at certain times of day, the apparent temperature of the object of interest can match the apparent temperature of the surrounding background, and the object can be very difficult to see in the thermal image. These events are referred to as thermal cross-over periods and typically occur twice a day, once after sunrise and again after sunset, but can occur at other times depending on ambient conditions. Polarization excels in this situation. Though polarization measurement does not require intensity or thermal contrast, any thermal signature that is present is also detected. LWIR thermal and polarization are combined in a single camera so that together the camera provides advantages over conventional thermal imagers in detection applications.

1.2 Polarimeter architectures

The specific configuration of an imaging polarimeter depends on a number of design requirements which, in turn, is dependent on the application and the state-of-the-art technologies available to meet those requirements. The physical configuration can be broken into categories[2] according to the optical path and layout of the electro optical components. There are five primary configurations for imaging polarimeters: rotating element of division of time, division of amplitude, division of aperture, micro-optic or division of focal plane, and channeled instruments. For this scenario in which the scene is dynamic with wave action and the sensor and / or the sensor platform may be moving, the division of focal plane approach is the one implemented in the Pyxis handheld polarimeter.

Recent advances in micro-optics manufacturing have allowed the integration of micro-optical polarization elements directly onto a focal-plane-array (FPA), thus creating a **"Division of Focal Plane"** (DoFP) polarimeter. In this configuration, pixelated linear polarization elements are attached intimately to the FPA. Several systems operating in the visible, SWIR, and LWIR waveband have been built using this technology. Most DoFP systems use interlaced polarization super-pixels as shown in Figure 4. A typical system must compute the Stokes vector at interpolation points on the FPA, thus DoFP systems must trade-off spatial resolution for polarimetric information. It should be noted that the intensity information is still collected at the full resolution of the FPA. DoFP systems have some significant advantages. All polarization measurements are made simultaneously for every pixel in the scene and it uses a single FPA with no added complications to the optical train. The architecture is very similar to commercial color cameras that use a Bayer color filter overlay on the FPA.

The polarization imagery is represented as Stokes images

$$s_0 = \frac{1}{2}(I_H + I_V)$$

$$s_1 = I_H - I_V$$

$$s_2 = I_{45} - I_{135}$$

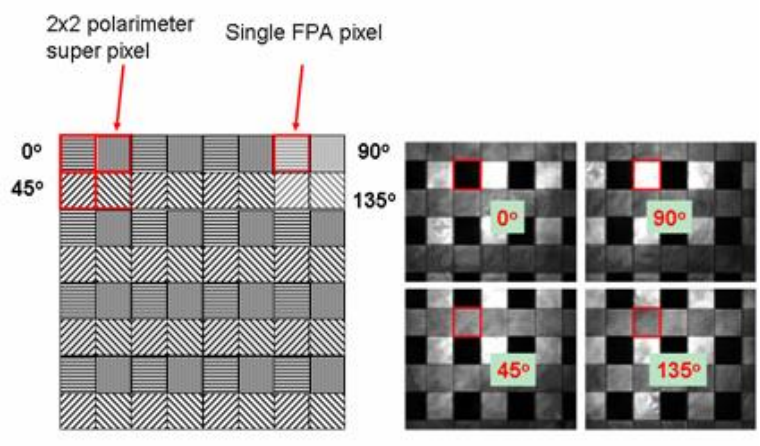

Figure 4. Polarization Elements of a Pixelated Imaging Polarimeter

where I_H,I_V,I_{45},I_{135} are images linearly polarized in the Horizontal, Vertical, 45° and 135° orientations. Note that the s_o image is simply the standard thermal image. The s_1 and s_2 images are often useful data products in and of themselves to view. However, additional data products derived from these three are often selected. For example, the degree of linear polarization (DOLP) image is often used to suppress background to detect an object. DOLP is given by,

$$DOLP = \sqrt{{s_1}^2 + {s_2}^2}.$$

Finally, data fusion is possible exploiting both the thermal and polarization data products. The imagery can be viewed independently or fused images can be formed from combinations. Data fusion captures all of the information and displays it in a single imager, giving the operator a more intuitive view of the scene. One of the preferred methods for displaying thermal and polarization together is called color fusion. Figure 5 shows a color-fused image taken with the Polaris Pyxis LWIR imaging polarimeter. In the color fused image, the un-polarized thermal image is displayed as normal grey scale. The polarization is displayed in color from a user defined threshold. A typical threshold is 1% DOLP. When a pixel exceeds 1% DOLP, the pixel is colored based on the orientation of linear polarization. The saturation of the color increases with increasing DOLP. For oil on water detection, this fusing capability tends to highlight the oil with color while still providing context through the gray scale IR image information.

Figure 5. LWIR color fused image of a vehicle. For thermal imagery, the color fuse enhances thermal information and is therefore dubbed eTherm®.

2. SENSOR HARDWARE

2.1 Pyxis description

Measurement of this polarimetric phenomenology requires capturing images with polarization filters. The approach chosen here is based on the Division of Focal Plane (DoFP) polarimetric architecture for imaging polarimeters. In this architecture, a pixelated polarizer array is attached to the FPA just above the sensing plane of the FPA (within a few microns). For infrared applications, the pixelated polarizer array uses an IR substrate such as silicon, germanium, or zinc selenide. A metal layer is deposited on the substrate and then the wire grid pattern is etched in to the metal layer using standard semi-conductor processing techniques creating the wire grid pattern. For the Pyxis, the substrate is silicon and the metal wires are aluminum. The polarizers are oriented at 0º and 90º, 45º and 135º, (left to right, top to bottom). Figure 4 (left) shows a schematic of the pixelated polarizer array. The pixels in different polarization states in a DoFP imaging polarimeter are combined to determine the polarization state of each pixel. A super-pixel is comprised of a 2x2 array of pixels. Figure 4 (right) shows the response of a larger segment of the pixelated polarizer array to vertically linearly polarized light. With vertically polarized light (90º orientation) incident, the horizontally polarized pixel is dark, the vertically polarized pixel is light and the 45º and 135º polarized pixels are gray. The measured incident polarization state is determined based on a weighted sum of interpolated pixels. It is important to note that both thermal and polarization images are captured at the full resolution of the array – spatial resolution is not lost. DoFP systems have the significant advantage that all polarization measurements are made simultaneously for every pixel in the scene. In addition, since the polarization sensitivity is integrated on the FPA, no additional optics are added to the optical train and the system is no larger and is equally rugged as a conventional camera.

One important measure of performance for a polarimeter is the Noise Equivalent Degree of Linear Polarization or NeDOLP. The NeDOLP is the rms noise of the reported degree of linear polarization for an un-polarized scene averaged across all operating pixels of an imaging polarimeter. It gives an indication as to what level of polarization signature is detectable by a polarimeter. Cooled LWIR polarimetric sensors can achieve below 0.1%. The Pyxis typical NeDOLP is around 0.3%.

Two models of Pyxis are shown in Figure 6. The Pyxis 640 LWIR-A model on the left which is not ruggedized but computes the polarization data products in an on-board processer and outputs processed analog polarization and thermal imagery and the raw digital data. The ruggedized version on the right, the Pyxis 640 LWIR–GR, outputs unprocessed digital data through a Gigabit Ethernet cable for processing on a laptop or tablet. The specifications are given in Table 1. Note that the noise equivalent noise parameters assume an f/0.85 lens, a faster lens than is usually used for microbolometer performance. Since the polarizer has lower throughput for unpolarized light, the loss of light is made up for through the use of a faster lens. However, with the faster lens, the sensor performance for the S_0 or radiometric imagery is similar to that of a (non-polarimetric) microbolometer.

Figure 6. The Pyxis 640-A panel and the Ruggedized GigabitEthernet models. Both analog and digital outputs are available on the -A. The buttons provide user selectability for the NTSC analog output.

Table 1. Pyxis Specifications

Detector	Uncooled VOx Microbolometer Array
Waveband (microns)	7.5-13.5
Pixel Pitch (microns)	17
Resolution (H x V pixels)	640 x 512
Camera Frame Rate (Hz)	7.5 or 30 Hz
Full Frame Pixel Operability	99.9%
Image products (from analog output, -A model only)	Radiance, S1, S2, DoLP, Orientation, ColorFuse, 14-bit raw
NEDT @ f/0.85	< 50 mK
NEDoLP @ f/0.85	< 0.5%
Size w/o lens (LxWxH in inches)	1.79 x 1.75 x 1.79
Weight w/o lens (g)	83
Input voltage (DC)	5
Steady state power @ 23° C (watts)	4
Peak power @ 23° C (watts)	5.3
Data interface	NTSC and 14-bit Camera Link standard GigE or LVDS optional
Lens Options (focal length, f/#)	20 mm, f/0.85 25 mm, f/0.86 50 mm, f/0.86

2.2 Sensor configurations and software

The Pyxis "core" is the sensor focal plane with an LVDS output and serial communications for setting sensor parameters. Several options exist for output configurations. These have been detailed elsewhere but in short, there are three different models. The Pyxis 640-A provides Camera Link and NTSC analog video out, the Pyxis 640-G replaces the -A back panel with one that only has an RJ-45 connector, and the -GR is a ruggedized version of the -G both of which give camera output and control over a Gigabit Ethernet connection. No analog polarization data products are available as output directly from the camera. The Pyxis 640-GR is the ruggedized version of the Pyxis 640-G and is shown in Figure 6 on the right. The case and cord are configured for IP67 environmental ruggedization but is otherwise operationally identical to the –G version. Multiple mounting points ease the use of the elongated case. In particular, mounting points on the bottom can be used to mount the sensor to a tripod or to a Picatinny rail which enables multiple mounting points include a hand grip.

All versions of the camera interface to a computer (or tablet) and use the Pyxis Vision Science (PVS) software framework developed by Polaris for commercial applications. PVS provides the ability to control the sensor, view the raw and processed sensor data, and record data for future processing. Note that the user interface provides a suite of standard color palettes, as well as toolbar buttons for selecting standard output imagery products. PVS gives the operator easy access to intensity data (temperature and radiance) as well as Stokes Vector polarimetry and degree of linear polarization (DoLP). The user has the ability to measure the value of a specific pixel, or to create a histogram or strip chart which displays the values for regions of interest within the image.

PVS is a software framework which provides certain standard functionalities such as display and data recording, with customization for user control of sensor specific operational parameters such as sensor calibration parameters such as non-uniformity correction (NUC) data calibration, and custom processing of sensor raw data for display and analysis. Normal operation of the PVS software can be divided into two basic functionalities: sensor operation, and data reduction. The operator is able to display the current video imagery being returned by the sensor when operating either way, but the focus of the sensor operation mode is in configuring the sensor for the task at hand, calibrating the sensor, and collecting the raw data of the event of interest. Processing priority is given to receipt and recording of the raw data frames, and display update rate is given less priority in order to ensure that all raw data is safely stored on the host computer. PVS allows the user to determine the method of data recording. Raw data may be streamed to the disk by the user manually using the graphical data recorder interface. The user may also choose to use the scripted Periodic & Event Recorder which allows for a great deal of flexibility in how data is recorded. Using the Periodic & Event Recorder the user defines a sequence of Record Windows. These Record Windows define the frame rate and number of frames to record. The Periodic & Event Recorder will execute these windows periodically or at user specified times. The Periodic & Event Recorder allows the

user to collect only that data that is of critical importance without having to store terabytes of data or having to be present with the sensor to manually record the event.

In data reduction mode the user loads a raw data file, and is able to play back the data for visual analysis, or to process the raw data into polarimetric or hybrid thermal/polarimetric data files. This processing can be performed on entire data sets, or, if the raw data files are large, can be performed on a subset of the raw data file which contains features or events of interest. These processed data files can be stored in numerical format for further analysis using external tools, or can be exported to standard video file format. Processing of the raw data can be performed as an offline activity after the data collection effort is complete. The algorithms which are used to compute the processed data files are coded in the C++ programming language as a library, and linked with the PVS software.

3. OHMSETT TESTING

In July of 2016, Polaris was invited to participate in a week of oil spill detection tests at Ohmsett sponsored in part by the ExxonMobil Upstream Research Company, an ExxonMobil subsidiary that engages in research and development of technology for exploration, development, production and gas commercialization. The test matrix consisted of two days of testing in a small, 1,000 gallon "fast tank" placed on the deck of the larger facility and then two and a half days of testing in the large 2 million gallon tank. The test objectives were to determine the effectiveness of IR polarimetric imaging for the detection of oil on water as compared to thermal imaging, to assess the sensitivity of the technique relative to oil thickness, look angle, and temperature changes, to establish night time detection capability, and to determine the effect of waves on the detection technique.

During the fast tank testing, initial polarimetric and thermal data was collected on oil samples with varied and known thicknesses of oil; time lapse, overnight imagery was collected to directly compare polarimetric and thermal response as the oil and water temperatures varied due to solar loading and night time radiative cooling; and angle dependent data was collected by varying the look angle relative to the tank. (Understanding of the angle sensitivity is important for optimizing placement of the sensor when deployed on ships, platforms, or unmanned aerial systems.) Figure 7 shows the fast tank placed on the deck next to the large tank and the oil-containing bins with the Pyxis camera mounted on a man lift.

Here we report on the results of the time lapse overnight testing. The results from this test are important for several reasons. First, the ability to detect and track an oil spill in darkness could significantly increase the effectiveness and efficiency of response to a spill. This ability would also enable monitoring around drilling operations, transfer points, and ports and harbors and enable spill detection at the earliest possible time. Second, thermal cross-over events resulting from changes in apparent temperature of the oil relative to the water creates periods when the oil and water are in thermal equilibrium and therefore the oil is essentially invisible in thermal imagery. These cross-over events typically happen several hours after sunset and sunrise.

Figure 7. "Fast tank" test setup for thickness, angle, and overnight testing. The view on the right shows a close up of the bins viewed by the sensor placed on the man lift. The bin on the left was filled with water and 1000 mL of oil resulting in an oil thickness of 5 mm and the bin on the right was filled with water and 100 mL of oil giving a thickness of 0.5 mm. The water level in the fast tank was just below that of the lip of the bin to keep a fairly pristine water background for comparison.

Figure 8 shows a sequence of the image data from the visible camera (left), the thermal output from the Pyxis camera (center) and the polarimetric image from the Pyxis camera (right). The view is roughly eastward looking. One second (30 frames) of this imagery was collected every ten minutes from 3 pm on July 26th, 2016 until 9 am the next morning. The time of the imagery shown in the figure is in the upper left corner of each row. The visible image shown at 21:27 is dark because there was no ambient illumination of the scene. Underneath these images is a time correlated plot of the contrast ratio (*CR*) of the polarimetric and thermal measurements of each bin relative to the water background where the yellow vertical lines are placed at the appropriate time stamp. A variant of the T-test contrast metric was used here where the oil is denoted by *O*, the water background is denoted by *B*, temperature is denoted by subscript *T* and polarization is denoted by subscript *P*. The contrast ratios for the thermal data (CR_T) and for the polarization data (CR_P) are then

$$CR_T = \frac{|O_T - B_T|}{6\sigma_T} \qquad CR_P = \frac{|O_P - B_P|}{6\sigma_P}$$

where the quantities are the mean of regions of interest chosen in the oil and water portions of the image and σ is the spatial standard deviation of each image. The top two lines in the plot show the polarimetric contrast ratio for the left bin (thicker oil, blue or darker gray) and right bin (thinner oil, orange or lighter gray). The bottom two lines in the plot show the thermal contrast ratio for the left bin (thicker oil, green or lighter gray) and right bin (thinner oil, red or darker gray).

There are several points that bear mentioning. At the beginning of the data collect, the sun was behind a cloud as evidenced by the visible image, the thicker oil on the left is warmer than the water and the thinner oil is close to thermal equilibrium with the water background. The contrast in polarization is quite strong for both bins although there is some slight non-uniformity of the thinner oil due to the fact that it had recently been poured into the bin and had not evenly coated the surface. At 17:77, the shadow of the man lift is apparent in the visible image. Thermal cross over events occur when CR_T is close to zero and in this data set they occurred at roughly 8 pm and 7:45 am. The 21:27 image shows the thinner oil is still essentially at thermal equilibrium with the surrounding water while the thicker oil is very slightly cooler. At 7:57, the thicker oil has warmed substantially due to solar heating and shows good contrast while the thinner oil is still the same temperature as the surrounding water. By 8:57 the oil in both bins had started heating from the direct sunshine. Note that the contrast in the polarization images remained consistently strong throughout the night and in particular when the thermal contrast was low. The polarization signal is beneficial for detection for a large portion of the sequence.

Although the time lapse data shows good quantitative performance, it was desirable to perform testing in the large tank at Ohmsett to minimize non-water background and also to see the effect of waves on the signature. Two and half days of testing provided the opportunity to look at the uncontrolled spreading of diesel fuel and two types of oil in varying amounts, performance in both breaking and non-breaking waves, while the sensor was moving along the tank. Figure 9 shows the mounting location on the bridge tower and the view of the tank from the sensor location. The sensor was also mounted in front of the window of the cab on the bridge for some measurements.

Figure 10 shows visible, thermal, polarization and the eTherm® color fused imagery that combines the thermal and polarization information. Two types of crude oil and diesel fuel are apparent in the polarization image while the diesel is slightly less visible in the eTherm image and not at all visible in the visible or thermal images. Also as expected from the fast tank testing, the thermal contrast is significantly less than that of the polarization. It should be pointed out that the shallow tank and white bottom results in a light colored blue for the water making the oil fairly visible. In deeper open ocean, the water color will be much darker and hence reduce the visibility of the oil in the visible imagery.

Results of testing with non-breaking waves is shown in Figure 11. Again, diesel fuel and two types of crude oil were released into the tank. While it is not readily apparent in this image, the video shows a slight loss of signal on the back side of the waves in some cases that is not attributable to simple obscuration of the wave. In these cases, the angle is essentially grazing relative to the surface normal of that part of the wave and the signal is consequently reduced. Practically speaking, however, the slight loss of signal is not significant and it can be said that the detection works in the presence of non-breaking waves.

Figure 12 shows imagery of two crude oil types mixed together through wave action and in the presence of breaking waves. The foam from the breaking waves shows a higher effective temperature than the surrounding water due to surface roughness and effective emissivity changes. The scale for the polarization image is set so that the foam polarization signature is very close to zero and hence essentially depolarized. However, immediately around the foam, the signatures perform as before and the contrast is unaffected as can be seen in both eTherm and polarization images

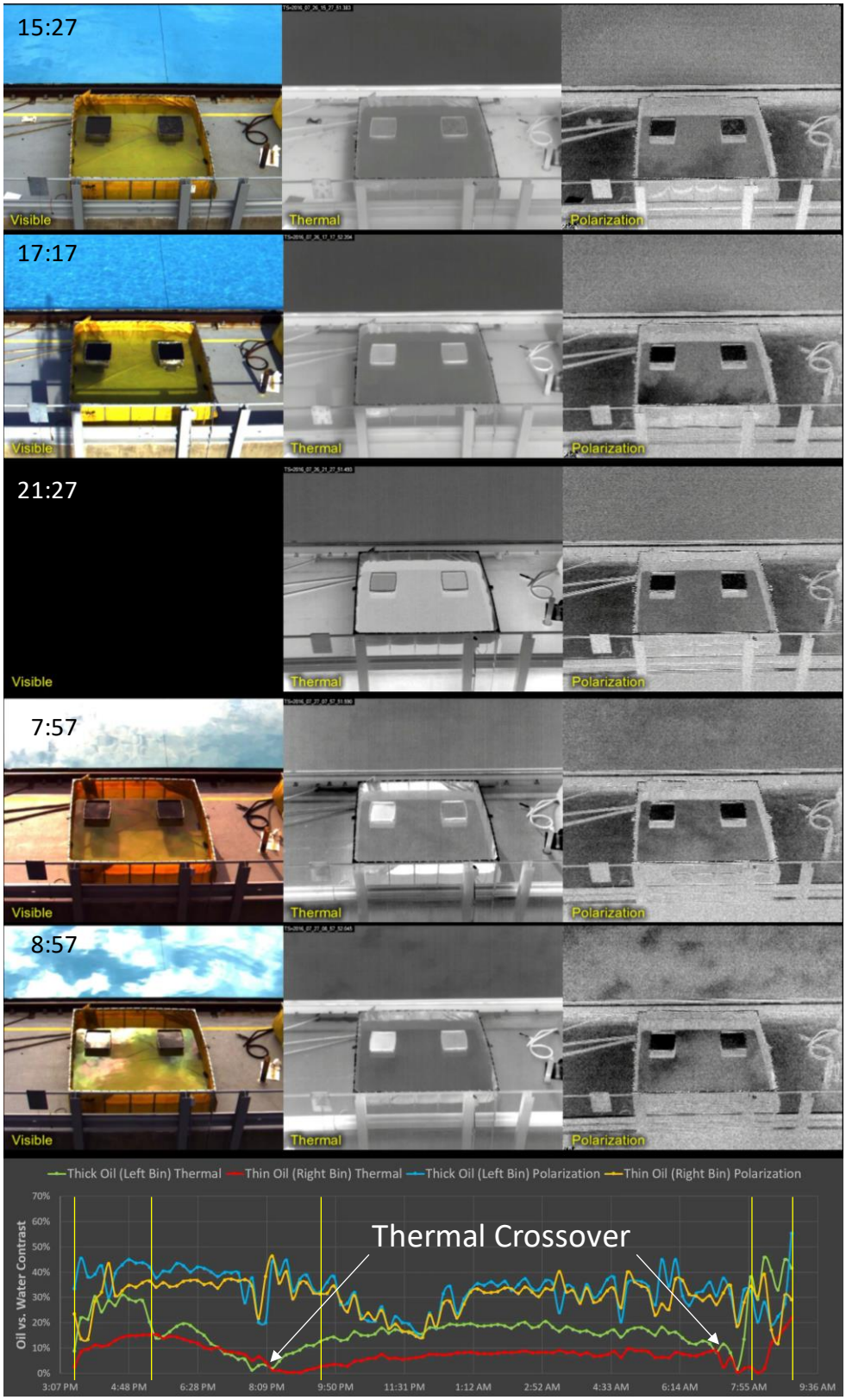

Figure 8. Time lapse, overnight imagery from the Fast Tank testing.

Figure 9. The moveable bridge over the Ohmsett tank. The Pyxis and visible camera were mounted on the tower at the right end of the bridge. The picture on the right shows the Pyxis and visible camera viewing the tank. Two small spills are visible about halfway down the tank. The wave machine was just started and the waves have almost propagated to the spills. The yellow fast tank is visible on the deck to the right side of the tank.

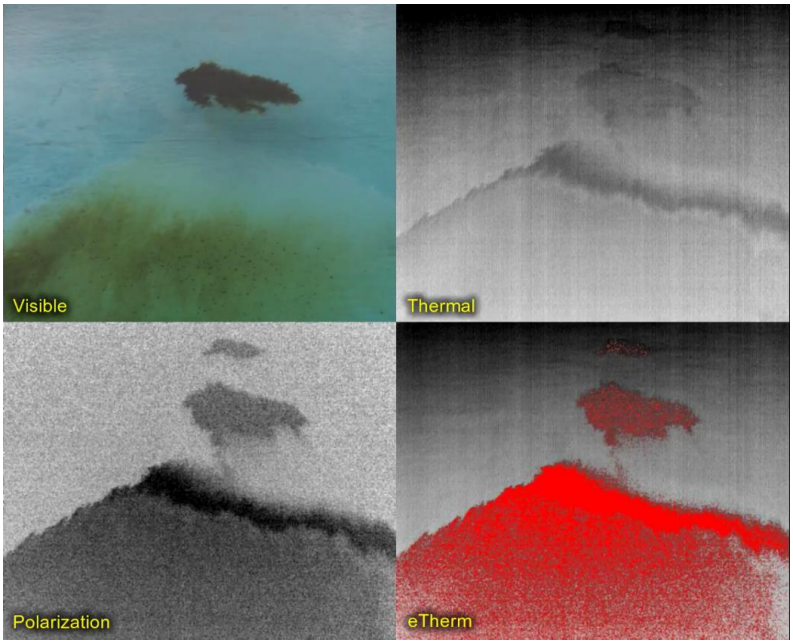

Figure 10. Visible (upper left), thermal (upper right), degree of linear polarization (bottom left), and eTherm fused (bottom right) polarimetric and thermal images of two crude oil types and diesel. The diesel is at the top of the image.

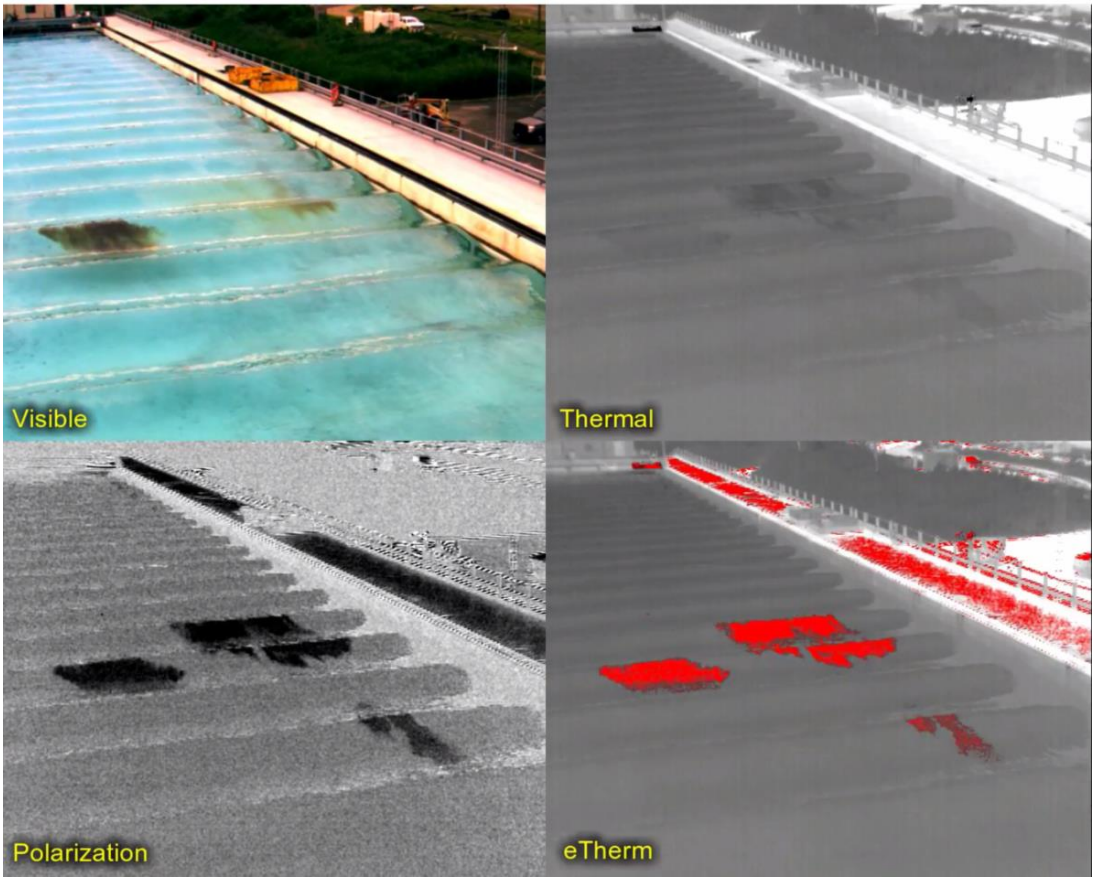

Figure 11. Visible, Thermal, Polarization and eTherm images. The two larger spots are two different types of crude oil. The smaller spill visible to the lower right in the polarization images is a 700 mL release of diesel. Thicknesses are estimated to range from 50 micrometers to 1 mm for the oil. For scale, the white colored deck to the right of the

4. SUMMARY AND FUTURE WORK

Thermal polarimetric imaging has been demonstrated to be very effective at detection oil and diesel spills at the Ohmsett test tank under a variety of conditions. The Pyxis LWIR 640 polarimetric camera was described as well as the phenomenology associated with thermal polarimetric signatures. Pyxis detected oil and diesel on the surface of the water with thicknesses of 50 micrometers, in waves, and at times of day in which the thermal signature underwent thermal cross-over. The signatures are strong enough and robust enough in various conditions that there is a strong possibility for automated detection for the oil and gas industry, for environmental monitoring, for ports and harbor surveillance, and other applications.

Work will continue to explore oil on water detection through infrared polarimetric imaging through measurement activities as well as through analysis and algorithm development. While one contrast metric was explored here, further approaches will be examined to ensure fair and accurate comparisons to conventional imaging techniques. This work will also be leveraged to establish and improve automated detection.

5. ACKNOWLEDGEMENTS

This work was funded in part through commercialization efforts under the Small Business Innovative Research (SBIR) program. Polaris testing at Ohmsett was sponsored in part by ExxonMobil Upstream Research Company.

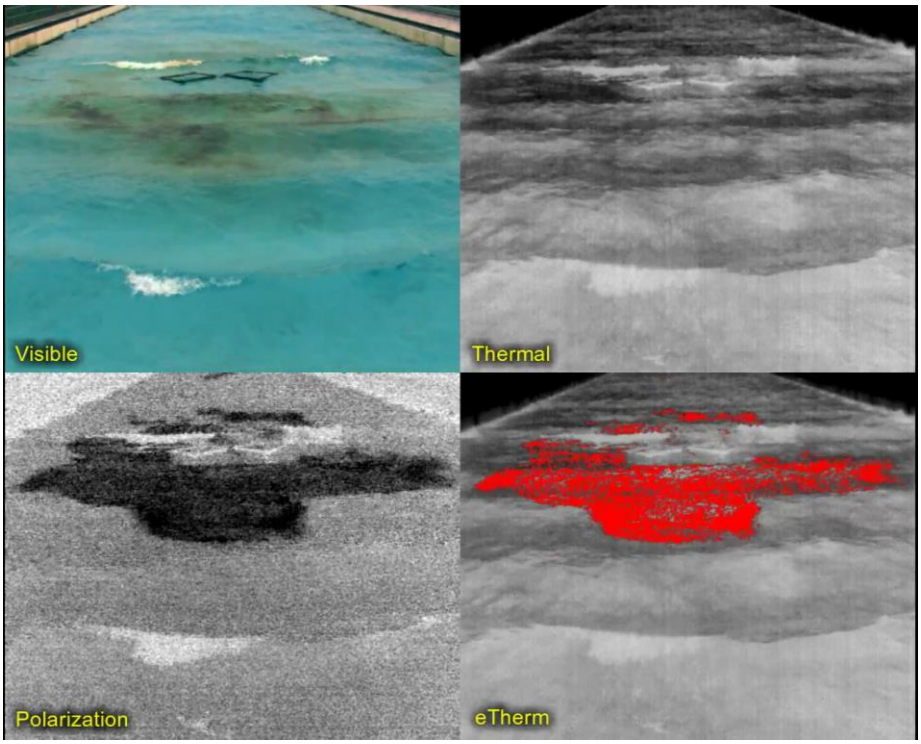

Figure 12. Visible, Thermal, Polarization and eTherm images in the presence of breaking waves. The signature detected here is a combination of two types crude oil mixed by the wave action. Foam from the breaking waves is white in visible, thermal and polarization imagery.

REFERENCES

[1] http://oilspill.skytruth.org, August, 2016.

[2] Felton, M., Gurton, K. P., Pezzaniti, J. L., Chenault, D. B., and Roth, L. E., "Measured comparison of the crossover periods for mid- and long-wave IR (MWIR and LWIR) polarimetric and conventional thermal imagery," Opt. Exp., Vol. 18. Issue 15, pp. 15704-15713 (2010).

[3] Felton, M., Gurton, K. P., Pezzaniti, J. L., Chenault, D. B., and Roth, L. E., "Comparison of the inversion periods for MidIR and LWIR polarimetric and conventional thermal imagery," Proc. SPIE 7672, (2010).